

A new alternative for corneal endothelial regeneration using autologous dental pulp stem cells

Begoña M Bosch

Universitat Internacional de Catalunya

Enrique Salero

University of Miami Bascom Palmer Eye Institute

Raquel Núñez-Toldrà

Imperial College London

Alfonso L Sabater

University of Miami Bascom Palmer Eye Institute

Francesc J Gil

Universitat Internacional de Catalunya

Roman A Perez (✉ rperezan@uic.es)

Universitat Internacional de Catalunya <https://orcid.org/0000-0002-0823-2303>

Research

Keywords: Cornea, dental pulp stem cells, neural crest, corneal endothelium, differentiation, cell reprogramming

Posted Date: July 24th, 2020

DOI: <https://doi.org/10.21203/rs.3.rs-45399/v1>

License: © ⓘ This work is licensed under a Creative Commons Attribution 4.0 International License.

[Read Full License](#)

Version of Record: A version of this preprint was published on January 28th, 2021. See the published version at <https://doi.org/10.3389/fbioe.2021.617724>.

Abstract

Background

Failure of the corneal endothelium cell (CEC) monolayer is the main cause leading to corneal transplantation. Autologous cell-based therapies are required to reconstruct in vitro the cell monolayer. For this purpose, we propose the use of dental pulp stem cells isolated from the third molars to form CEC monolayer. We hypothesize that by using dental pulp stem cells (DPSC) that share an embryological origin with CEC, as they both arise from the neural crest, may allow a direct differentiation process avoiding the use of reprogramming techniques, such as induced pluripotent stem cells (iPSC).

Methods

In this work, we report a two-step differentiation protocol, where dental pulp stem cells are derived into neural crest stem cells and, then, into CEC.

Results

Initially, we compared the efficiency of direct differentiation of DPSC with the differentiation of iPSC to express NCSC related genes in adhesion culture, showing significantly higher levels of early stage marker AP2 for the DPSC compared to iPSC. To provide better environment for NCSC gene expression, suspension method was performed, which induced the formation of neurospheres. The results showed neurosphere formation after few days, obtaining the peak of NCSC marker expression after 4 days, showing overexpression of AP2, p75 and CHD7 markers, confirming the formation of NCSC like cells. Furthermore, pluripotent markers Oct4, Nanog and Sox2 were as well upregulated in suspension culture. Neurospheres were then directly cultured in CEC conditioned medium for the second differentiation, showing the conversion of DPSC into polygonal like cells expressing higher levels of ZO-1, ATP1A1, COL4A2 and COL8A1 markers, providing proof of the successful conversion into CEC.

Conclusions

Therefore, our findings demonstrate that patient-derived dental pulp stem cells represent an autologous cell source for corneal endothelial regeneration that avoids actual transplantation limitations as well as reprogramming techniques.

Background

Corneal transplantation, known as keratoplasty, is the most frequently performed type of transplant worldwide, with over 185,000 procedures performed each year [1]. The main indication of corneal transplantation in the US is Fuchs dystrophy, a disease related to the innermost corneal layer, known as

corneal endothelium [2]. In fact, endothelial keratoplasties, where only the corneal endothelium is replaced, represent 60% of all corneal transplants, and this percentage is increasing every year [3]. The lack of donors, together with an increased demand for corneal tissue due to population aging, urges to find alternative solutions [1]. In this context, cell-based therapies are being developed in order to overcome actual limitations [1].

Considering that the corneal endothelium is the most replaced layer and that it consists of a monolayer of corneal endothelial cells (CEC), it is necessary to obtain such layered cell structure. Hence, the aim of these cell-based therapies related to CEC is to restore damaged endothelium by conforming cells *in vitro* with similar characteristics to those of native cells, using in most cases, cells obtained from donors. Nevertheless, this remains a great challenge as CEC have a restricted proliferative ability in humans, limiting its feasibility [4]. Furthermore, donor corneas are generally from older patients and these cells present even lower proliferation rates, being more prone to senescence than younger corneas [5–8]. In order to overcome the senescence state of cells, a recent study cultured CEC from a young donor and injected them with ROCK inhibitor, which has been described to reduce intraocular pressure, to increase CEC cell density and to promote the typical polygonal monolayer phenotype [9, 10]. The expanded cultured CEC from the donor were successfully placed in the host patient achieving increased cell densities after 24 weeks, which was ascribed to the ROCK inhibitor [10]. Despite of the recent efforts, patients still required local or systemic immunosuppression to prevent corneal tissue rejection, which is the main cause of corneal transplant failure. Consequently, an alternative autologous CEC source is required.

In this sense, recent studies have shown the use of somatic cells from the same patient to produce induced pluripotent stem cells (iPSC) that can eventually be differentiated into CEC [11]. Promising results have been achieved with these cells, mainly consisting of a two-step process based on the natural CEC embryological development from the neural crest (NC). This process consists in a first-step, where cells are differentiated into NC stem cells (NCSC) followed by a second-step, where NCSC are differentiated into CEC [12, 13]. Despite of the positive results, their clinical application is hindered due to safety issues. Furthermore, their production requires a previous tedious step in which cells are reprogrammed from somatic cells, mainly fibroblasts, into cells with a pluripotent status, requiring the use of gene transfection and long and expensive culture periods.

Hence, we propose the use of patient-derived dental pulp stem cells (DPSC) as an alternative approach for corneal endothelial therapy. DPSC can be easily obtained and cultured from third molars using a non-invasive technique, which avoids ethical and safety issues [14]. DPSC exhibit a great differentiation potential and have been differentiated into many cell types [15, 16]. Interestingly, DPSC, as well as CEC, arise from cranial NC and present similar characteristics to NC progenitor or stem cells [14, 17]. Some recent studies proposed as well the use of DPSC as a possible cell source, nevertheless these works were mainly related with the corneal epithelium or the stroma [18, 19]. Therefore, in this work we aim to determine if patient-derived DPSC, which share the same embryological origin with CEC, can be used as a

potential autologous source for corneal endothelial regeneration, which to the best of our knowledge, has not been previously proposed.

For doing this, we propose a two-step protocol, involving the dedifferentiation of DPSC into NCSC, followed by their subsequent differentiation into CEC. We hypothesize that the initial dedifferentiation process can overcome the limitations of the cellular reprogramming from initial somatic cells, mainly fibroblasts, into iPSC and their subsequent differentiation into NCSC, reducing cost time and avoiding safety issues [20]. In order to validate the hypothesis, iPSC are also being produced from DPSC, allowing the comparison of direct conversion from DPSC into NCSC as well as the differentiation from reprogrammed iPSC.

Methods

Dental pulp stem cells isolation and culture

Dental pulp was extracted for orthodontic reasons from human third molars of healthy patients. DPSC were isolated modifying a previous protocol [21]. Briefly, dental pulp was digested with 3 mg/mL collagenase I (Sigma-Aldrich) at 37°C for 60 minutes. Disaggregated pulps were washed with phosphate-buffered saline (PBS) (Sigma-Aldrich) and cultured in expansion medium at 37°C in a 5% CO₂ incubator. Cell expansion medium consisted of Dulbecco's modified Eagle's medium (DMEM) high glucose (Thermo Fisher Scientific) supplemented with 10% fetal bovine serum (FBS, Sigma-Aldrich), 1% GlutaMAX and 1% penicillin-streptomycin (Thermo Fisher Scientific). When DPSC reached 70% confluence, cells were detached using TrypLE™ Express Enzyme (Thermo Fisher Scientific) and re-plated or used for experiments. Cells were used until a maximum passage of 4.

Production of induced Pluripotent Stem Cells

Cell reprogramming with Sendai virus

For the reprogramming process, DPSC were reprogrammed using the CytoTune™ Reprogramming System, a non-integrating viral vector [22]. Briefly, cells were plated in a 6-well plate at a cell density of 1×10^5 cells/cm². After 48 hours, the transduction of the Yamanaka factors (Oct4, Sox2, Klf4 and c-MYC) was performed at an infection multiplicity of 3 using Sendai virus. Twenty-four hours after the transduction, culture medium was replaced with fresh media to remove the reprogramming vectors. Then, culture media was changed every other day. Total RNA was extracted at day 21 of the reprogramming process for PCR analysis. The results were compared to day 0, which was considered as the negative control.

As a control for the reprogramming process, human dermal fibroblasts were used (CIMA, University of Navarra). Fibroblasts were cultured in cell expansion medium at a cell density of 3×10^3 cells/cm². The

medium was changed every 2-3 days and when cells reached 70% confluence they were used for reprogramming process.

Reprogrammed cells in feeder and feeder-free conditions

One week after the transduction, the transduced cells were plated on feeder dishes, which provide an extracellular matrix needed for the maintenance of an undifferentiated state until the formation of iPSC colonies [23].

For the preparation of the feeder layer, mouse fibroblasts SNL 76/7 (Cell Biolabs) were prepared as indicated in the commercial protocol. Briefly, cells were cultured at a cell density of 2×10^4 cells/cm² in expansion medium adding 0.1 mM MEM non-essential aminoacids (Sigma-Aldrich). When cells reached 90% of confluence, they were inactivated using 10 µg/mL mitomycin C (Sigma-Aldrich) and resuspended in DMEM. After 2 hours, cells were washed three times with 1X PBS, then detached and used for experiments.

After 24 hours of culture in feeder layer, culture medium was changed to iPSC medium, which consisted of Knock-out DMEM/F-12 (Thermo Fisher Scientific), 20% Knockout Serum Replacement (Thermo Fisher Scientific), 0.1 mM MEM non-essential aminoacids, 0.1 mM 2-mercaptoethanol (Thermo Fisher Scientific), 4 ng/mL basic fibroblast growth factor (bFGF, Sigma-Aldrich), 1% GlutaMAX and 1% penicillin-streptomycin.

Finally, after three weeks of culture in feeder dishes, iPSC were detached using collagenase type IV (Thermo Fisher Scientific) and were adapted to feeder-free conditions using 10 µg/mL vitronectin-coated dishes (STEMCELL Technologies).

First step cell differentiation

Neural crest stem cells production

The DPSC dedifferentiation into NCSC was considered as the crucial step for the formation of CEC precursors. We followed a modified differentiation process based on our previous results, which consisted on culturing cells on adhesion conditions while using a differentiation medium [24].

In this adhesion method, DPSC dedifferentiation was compared with the differentiation of the previously described iPSC-derived from DPSC. Both DPSC and iPSC-derived from DPSC were incubated in NC induction medium at a cell density of 0.5×10^3 cells/cm² for 21 days. The NC induction medium consisted of DMEM-F12 (Thermo Fisher Scientific) supplemented with 1X B-27 supplement (Thermo Fisher Scientific), 1X N-2 supplement (Thermo Fisher Scientific), 20 ng/mL epidermal growth factor (EGF), 20 ng/mL bFGF, 5 ng/mL heparin (Sigma-Aldrich) and 2 mM L-alanyl-L-glutamine (Sigma-Aldrich).

Medium was changed every 2-3 days. In order to analyze cell phenotype, total RNA was extracted at day 21. RNA results were compared to day 0, which corresponds to undifferentiated cells.

After initially comparing the traditional iPSC differentiation method with our novel protocol, we then compared our adhesion culture differentiation protocol of DPSC with a suspension differentiation method. The suspension method consisted of a modification from a previously described protocol based on neurospheres (NS) formation [25]. For this purpose, DPSC were cultured on ultra-low adhesion 24-well plates (Corning) in the previously described NC induction medium at a cell density of 2×10^4 cells/well. Cells were forced to aggregate among them, forming NS-like structures. The culture was monitored by visual inspection using an optical microscope (Olympus CKX41, Nikon). The optimum size was considered to be below 250 μm in order to avoid hypoxia. The culture finalized once the desired NS size was reached. Total RNA was extracted every day of dedifferentiation for PCR analysis and was compared to day 0, corresponding to undifferentiated DPSC cells. The diameter of NS was measured at days 1, 2, 3, 4 and 5 of suspension culture using ImageJ software (U.S. National Institutes of Health).

Second step cell differentiation

Human corneal endothelial cell conditioned medium preparation

Six non-transplantable human corneoscleral rims were obtained from the Florida Lions Eye Bank (Miami, USA). Descemet's membrane and corneal endothelium were isolated as previously described with some modification [26]. Briefly, corneal tissue was rinsed with PBS. The iris and possible contaminations were removed with tweezers. Subsequently, the Descemet's membrane with the corneal endothelium were gently removed with tweezers and cultured in CEC medium at 37°C in a 5% CO₂ incubator. CEC medium consisted of DMEM high glucose (Thermo Fisher Scientific) supplemented with 5% FBS, 1% GlutaMAX, 2 ng/mL bFGF, 0.1 mM 2-mercaptoethanol, 10 ng/mL heregulin beta (Sigma-Aldrich), 10 ng/mL activin A (Miltenyi Biotec), 200 ng/mL IGF-I (Sigma-Aldrich) and 1% penicillin-streptomycin. Previous reports have demonstrated that conditioned medium enhanced cell differentiation [27,28]. Therefore, culture medium was replaced every 2 days, and was collected once CEC reached confluency. Collected medium (conditioned medium), was filtered (0.45 μm) and stored at -80°C in order to maintain its biological activity. Conditioned medium was used in the second step of cell differentiation.

Corneal endothelial cell differentiation

The previously obtained NCSC in the first step were used for the second step of differentiation. For this process, high cell density is needed in order to mimic the natural conditions in which CEC are found. For this purpose, once the NS were obtained, these were cultured for 15 days in adhesion conditions to allow cell expansion. Total RNA was extracted when NS were formed (day 4) and at the end of the expansion

process (day 19), in order to verify if the NCSC phenotype was maintained during the expansion process. RNA results were compared to day 0, which were undifferentiated DPSC cells.

Once the proper NCSC number was reached, regardless of the expansion method used, the conditioned medium from isolated human CEC was used to induce the differentiation into CEC. For this purpose, NCSC-derived from DPSC were cultured at a cell density of 2×10^5 cells/cm² for 15 days in conditioned medium. Conditioned medium was changed every 2 days. Total RNA was extracted at days 12 and 19 of differentiation for PCR analysis. As a positive control, RNA extracted from isolated CEC was used. Results were compared to day 0, which corresponded to undifferentiated DPSC cells.

The different cellular processes taking place in this study are summarized in Figure 1.

Cell morphology analysis

As an initial characterization, cellular morphology was analyzed. For this purpose, samples were fixed using 4% paraformaldehyde (Sigma-Aldrich) for 20 minutes at room temperature. Then, cells were washed with PBS and were observed by optical microscopy (Olympus CKX41, Nikon) to obtain an overall cell morphology.

Quantitative real-time reverse transcription polymerase chain reaction (qRT-PCR)

The relative expression of characteristic genes was analyzed to verify the differentiation process by quantitative real time – polymerase chain reaction (qRT-PCR). Total RNA was isolated using NucleoSpin RNA kit (Macherey-Nagel) and reversed transcribed into cDNA using Transcriptor First Strand cDNA Synthesis Kit (Roche) following the manufacturer's indications. Specific primers, shown in Table 1, and FastStart Universal SYBR Green Master (Roche) were used to amplify the cDNA. Lastly, a CFX96 real-time PCR Detection System (Bio-Rad) was used for the quantitative real-time PCR process.

Table 1. List of primers used for cDNA amplification in quantitative RT-PCR.

| Gene | Primer | Sequence (5' -3') | Accession Number |
|---------|---------|----------------------------|------------------|
| Oct4 | Forward | AGCGAACCAGTATCGAGAAC | NM_002701 |
| | Reverse | TTACAGAACCACACTCGGAC | |
| Nanog | Forward | TGAACCTCAGCTACAAACAG | NM_024865 |
| | Reverse | TGGTGGTAGGAAGAGTAAAG | |
| Sox2 | Forward | GCCGAGTGGAAACTTTTGTCTG | NM_003106 |
| | Reverse | GGCAGCGTGTACTTATCCTTCT | |
| p75 | Forward | CCTACGGCTACTACCAGGATG | NM_002507 |
| | Reverse | CACACGGTGTCTGCTTGT | |
| AP2 | Forward | AGGTCAATCTCCCTACACGAG | NM_003220 |
| | Reverse | GGAGTAAGGATCTTGCGACTGG | |
| CHD7 | Forward | TGATGAGTCTTTTGGCGAGG | NM_017780 |
| | Reverse | CTGGATTTTCCGGGTAACCAC | |
| Sox10 | Forward | CTGGACACTAAACCCCTGCC | NM_006941 |
| | Reverse | CATGTGGACTGGGCTGCAGAC | |
| ATP1A1 | Forward | TGTGATTCTGGCTGAGAACG | NM_001160234 |
| | Reverse | TGCTCATAGGTCCACTGCTG | |
| COL4A2 | Forward | TAAGGGTGAAAAGGGTGACG | NM_001846 |
| | Reverse | ACTGATCTGGGTGGAAGGTG | |
| COL8A2 | Forward | GAAGTGGACGGTTCTGTGGT | NM_003759 |
| | Reverse | AATTGCCGAAAGAGCTTGAA | |
| ZO-1 | Forward | AGTTTGGCAGCAAGAGATGG | NM_001355015 |
| | Reverse | GCTGTCAGAAAGATCAGGGA | |
| GAPDH | Forward | CTGGTAAAGTGGATATTGTTGCCAT | NM_002046 |
| | Reverse | TGGAATCATATTGGAACATGTAAACC | |
| b-ACTIN | Forward | AGAGCTACGAGCTGCCTGAC | NM_001101 |
| | Reverse | AGCACTGTGTTGGCGTACAG | |

Statistical analysis

Mann-Whitney U-test was used to analyze significant differences. Differences with a P value of less than 0.05 were considered statistically significant.

GraphPad Prism version 6 (GraphPad Software Inc.) was used to graph the quantitative data presented as mean and standard deviation (SD). Statistical analyses were carried out using Statistical Package for the Social Sciences (SPSS) 21 (IBM).

Results

Production and characterization of induced Pluripotent Stem Cells

The production of iPSC was performed to analyze whether the pluripotent like status is required for the production of NCSC or a direct conversion from DPSC into NCSC is a plausible route. These iPSC were obtained from DPSC as well as from the well-established fibroblasts, which were used as positive control. Both cell types were transduced using Sendai virus with the four Yamanaka factors. After two weeks of the transduction, first emerging iPSC colonies started to appear, observing how cells started to change its spindle-like morphology into a more rounded morphology. In order to validate that the cells were correctly reprogrammed, pluripotent expression was evaluated. Results showed that cells reprogrammed from DPSC presented statistically significant higher levels of gene expression of the pluripotent markers Oct-4 and Nanog compared to the non-reprogrammed cells as well as to the positive control, as shown in Figure 2A.

Colonies were carefully picked at week 4 post-transduction and were expanded in feeder conditions for at least four more weeks. Adaptation to feeder-free conditions, on vitronectin-coated dishes, was performed 8 weeks after transduction. iPSC on vitronectin-coated dishes presented pluripotent like characteristics such as the formation of cobblestone-like colonies, presenting individual cells with a high nuclear to cytoplasm ratio (Fig. 2B).

Cell differentiation

Neural crest stem cells production

We first evaluated the formation of NCSC using adherent conditions. Regarding the overall cell morphology, cells presented a more stellate typical morphology at day 21 of differentiation when the differentiation was performed from iPSC (Fig. 3A). In contrast, dedifferentiated cells from DPSC exhibited a more elongated morphology after 21 days of dedifferentiation (Fig. 3A).

Aiming to analyze the fold gene expression, in the case of NCSC-derived from iPSC, surprisingly, the NCSC markers AP2 and p75 decreased throughout the differentiation process (Fig. 3B). However, in the case of NCSC-derived directly from DPSC, dedifferentiated cells presented statistically significant higher levels of the early NCSC marker AP2, whereas the mid-term marker p75 was down-regulated at day 21 of the dedifferentiation (Fig. 3B).

In order to induce a higher cell-to-cell interaction, the suspension culture was performed. Ideally, the cell-to-cell contact could help mediate in higher NCSC induction capability. Therefore, we cultured DPSC for 5 days in suspension culture plates. Floating clusters or cell aggregates started to appear at day 1 and their diameter increased until day 5 (Fig. 4). As excessive NS diameters were hypothesized to induce hypoxia, limiting as well the diffusion of nutrients in the center of the NS, its diameter was monitored to prevent excessive NS sizes. As shown in Figure 5, at day 1, cell aggregates presented values of NS below 70 μm . The NS size progressively increased during the next days and presented an average diameter of 100 to 150 μm at days 2, 3 and 4. At day 5 of culture, the number of NS present in the culture abruptly decreased

presenting a significant number of floating cells in the culture. Moreover, the diameter of the NS at day 5 was excessively big, being around 300 μm .

To further characterize the dedifferentiation process, fold gene expression was evaluated in order to obtain the optimal peak day of the process. The analysis of NCSC markers (Fig. 6A) showed that the early transcription factor AP2 exhibited its peak level at day 3, not presenting statistically significant differences with day 2 and day 4, while p75 and CHD7, presented the highest expression levels at day 4, presenting significant differences with the other culture days. Interestingly, pluripotent markers Oct4, Nanog and Sox2 showed as well a significant increase with time, showing its peak level at day 4 of dedifferentiation (Fig. 6B).

Once the optimal peak day of NS formation was determined, NS were then cultured on adherent conditions for 15 days more in order to obtain larger amounts of NCSC. As shown in Figure 7A, cells migrated from the NS, allowing the diffusion of cells from the original NS, hence disrupting its morphology. These migrated NC cells, reached confluence after 15 days of expansion (Fig. 7A). In order to confirm that NC migrating cells were able to maintain NCSC phenotype, gene expression levels were analyzed (Fig. 7B). The pluripotent markers were evaluated to verify if the increase of the cell-to-substrate interactions overruled the cell-to-cell interactions and hence reduced the pluripotent expression. Regarding this, as shown in Figure 7B, the different markers Oct4, Nanog and Sox2, were significantly up-regulated during the initial suspension culture (day 4) while its expression was down-regulated at the end of the expansion culture (day 19). Similar results were obtained with the early NCSC markers AP2 and Sox10, showing an initial up-regulation followed by a down-regulation at day 19. The levels of AP2 decreased to values similar to those at day 0 (Fig. 7B). In contrast, the expression of the mid-term NCSC marker p75 presented an increase expression throughout the expansion process, obtaining its highest expression at day 19 (Fig. 7B).

Corneal endothelial cell differentiation

The second step of differentiation was to culture NCSC-derived from DPSC, corresponding to day 4 of dedifferentiation, in corneal endothelial conditioned medium for 15 days more. Cell morphology was observed with optical microscopy, showing that cells started to exhibit a polygonal morphology characteristic of CEC at day 12 of differentiation and this was maintained until the end of the differentiation process, corresponding to day 19 (Fig. 8A).

Finally, we compared the values of different CEC markers during the differentiation process. As shown in Figure 8B, the gene expression of the typical CEC marker Zona Occludens-1 (ZO-1) showed a significant increase at days 12 and 19 of the differentiation. Moreover, the Na⁺/K⁺-ATPase pump ATP1A1 expression showed a significantly progressive increase at days 12 and 19 (Fig. 8B). Lastly, extracellular matrix components as collagen type IV and VIII (COL4A2 and COL8A2) were as well analyzed, and its expression significantly increased at days 12 and 19 of differentiation compared to day 0 (Fig. 8B).

Although ZO-1 exhibited similar values to the control sample, which were freshly isolated CEC from donor corneas, the other markers presented decreased levels of gene expression (Fig. 8B).

Discussion

New cell therapies are needed for corneal endothelial regeneration in order to overcome problems related to corneal transplantation, which is the gold standard, such as global scarcity of healthy donor corneas or corneal tissue rejection [29]. Dental pulp represents a very accessible source, as it contains stem cells with similar characteristics to NCSC due to their NC origin [14]. In the same way, CEC also derive from the NC [17]. Therefore, in the present study, we have evaluated the feasibility of obtaining CEC from patient-derived DPSC, which could be used to treat corneal endothelial dysfunction using a safe and accessible source of autologous cells.

Based on previous protocols [30, 31], our differentiation process consisted of a two-step differentiation protocol, where DPSC were dedifferentiated into NCSC and, finally, into CEC. As the gold standard differentiation is the use of pluripotent stem cells as the cell source, we initially reprogrammed DPSC into iPSC in order to compare and validate the differentiation process of both cell types.

Interestingly, our preliminary results showed that the gene expression of the pluripotent markers Oct4 and Nanog in reprogrammed cells derived from DPSC presented significantly higher levels than the positive control, which were fibroblasts (Fig. 2A). This difference could be due to the later development in time of the DPSC, which are isolated from third molars, compared to fibroblasts, which are differentiated cells. In fact, DPSC endogenously express some pluripotent markers [32], which has been described to enhance the reprogramming process [33–35]. Therefore, the generation of iPSC seems to be easily performed and with higher pluripotent expression when using DPSC compared to fibroblasts. Furthermore, reprogrammed cells exhibited its typical cobblestone morphology with an elevated nuclear to cytoplasm ratio (Fig. 2B), as described by other groups [36, 37].

Once iPSC-derived from DPSC were successfully generated, we then compared the conversion potential of iPSC and DPSC into NCSC. It was previously reported that iPSC could be differentiated into NCSC using an adherent culture [24]. Therefore, we used this strategy as a first approach for the formation of NCSC. Optical microscope images (Fig. 3A) showed that the differentiation from iPSC exhibited cells with a stellate morphology typical for NCSC, similar to previous reports [25, 38], while the dedifferentiated cells directly from DPSC presented a more elongated shape (Fig. 3A). Surprisingly, in the dedifferentiation process from DPSC into NCSC, the gene expression of typical NCSC markers showed that AP2 presented a significant up-regulation compared to the NCSC obtained from iPSC (Fig. 3B). This could be related with the fact that undifferentiated DPSC already express NCSC markers, as previously demonstrated [32]. For this reason, the formation of NCSC may be accelerated using DPSC compared to iPSC, which may need longer time of NC induction conditions for a complete differentiation. As DPSC seem to successfully generate NCSC, and in order to reduce time and costs, our next strategy was only performed using DPSC.

We then evaluated if a suspension culture, which mimics the embryological process of gastrulation and promotes cell-to-cell interactions [39], could further enhance the formation of NCSC. As shown in Fig. 4, this system promoted the formation of cell aggregates at day 1. However, these cell aggregates that measured around 50 μm of diameter were not considered NS as its sizes range normally from 100 to 200 μm , as was previously reported [40]. NS between these sizes were already formed at day 2 of culture (Fig. 5) and their size progressively increased at longer days of culture. However, at day 5 of culture, NS started to disrupt its morphology and cell survival decreased, which was probably ascribed to a lower nutrient and oxygen diffusion into the NS inducing cell death. This is in accordance with a previous report which concluded that above 250 μm the diffusion of nutrients and oxygen is very limited [40]. Therefore, gene expression was evaluated from day 0 until day 4 in order to confirm the formation of NCSC (Fig. 6). Interestingly, the gene expression of pluripotent markers such as Oct4, Nanog and Sox2 (Fig. 6B) showed an increasing expression throughout the different days of culture. This can be related with enhanced cell-to-cell interactions in the suspension conditions which could stimulate the beginning of gastrulation, which occurs in the earlier weeks of embryogenesis and hence presents the highest levels of pluripotency [39]. Furthermore, the expression of the NCSC marker AP2 exhibited its peak before day 4, while the expression of p75 and CHD7 presented its higher fold expression at day 4 of dedifferentiation. These results were in accordance with our initial hypotheses, as AP2 is a transcription factor that is expressed as an early inductive signal, whereas p75 and CHD7 are mid-late markers expressed in the migratory NC [38, 41]. Based on these results, we selected the suspension method for the formation of NCSC.

Prior to the formation of CEC (second-step of differentiation), which requires an initial high cell density, there was a need to expand the NS in adherent conditions. As deduced from the suspension culture, optimum culture time was established to be 4 days. In this sense, it was important to verify if culturing the NS in adhesion after their formation could provide enough number of cells with adequate phenotype. Our results showed (Fig. 7B) that the expression of pluripotent markers and NCSC markers, AP2 and Sox10, decreased during the adherent expansion (day 19). These results are in line with a previous study that determined that pluripotent markers were inherently decreased in adherent culture [42], which is related to the fact that the cell-to-matrix contact increased while the cell-to-cell interaction decreased. However, the expression of the NCSC marker p75 increased during the adherent expansion culture. It has been described that p75 is related to migratory NC cells [38] and, therefore, it is expected to present higher levels during the expansion culture. Therefore, we determined that NCSC expansion using an adherent culture was not viable due to the altered phenotype and hence the optimum culture was to increase the initial number of DPSC in culture to obtain a sufficient number of cells using the suspension method for the subsequent differentiation.

Finally, once the first-step of the differentiation was achieved and confirmed, NCSC-derived from DPSC were differentiated into CEC. Other groups have determined that the culture with conditioned medium promotes the formation of CEC [28, 43], so the use of conditioned medium from freshly isolated CEC was evaluated to induce the differentiation of NCSC-derived from DPSC. Optical microscope images showed that cells started to exhibit its typical polygonal morphology at day 12 of differentiation (Fig. 8A), indicating that the differentiation process had already started, and was maintained until day 19. We then

characterized the differentiated cells by gene expression, using characteristic CEC markers ZO-1, ATP1A1, COL4A2 and COL8A2 [44]. As shown in Fig. 8B, we identified higher levels of expression at days 12 and 19 of CEC differentiation of the tight junction ZO-1, the pump function ATP1A1, and the extracellular collagens COL4A2 and COL8A2, compared to undifferentiated DPSC, indicating that cells were correctly differentiating into CEC. Although the gene expression was higher in CEC-derived from DPSC, its value was lower than the expression of human CEC, used as control. This is in line with a previous study which presented lower levels of gene expression of CEC-derived from ESC compared to human CEC or CEC cell line [30, 45].

Despite the described protocol has shown positive results and might significantly reduce cost and time of production, the differentiation process does not mimic the native environment of CEC such as the natural curvature of the cornea, the *in vivo* cross talks or the specific extracellular matrix composition. Further experiments mimicking these native conditions should enhance the expression of differentiated CEC into levels of expression similar to isolated CEC.

Conclusions

In our work, results have shown that patient-derived DPSC can be successfully de-differentiated into NCSC using a short-time suspension culture, through the formation of NS. The dedifferentiated cells exhibited self-renewal and multipotent abilities and expressed characteristic NCSC markers. Furthermore, NCSC-derived from DPSC cultured in conditioned medium were able to generate CEC, which share characteristics with native CEC such as polygonal morphology and high expression of typical markers at the end of the differentiation. All in all, this project presents a rapid and simple protocol for the formation of NCSC from patient cells, which can be used for the formation of CEC. The generation of patient-derived CEC would overcome actual problems of corneal endothelial regeneration.

Abbreviations

CEC
corneal endothelial cells
DPSC
dental pulp stem cells
IPSC
induced pluripotent stem cells
NC
neural crest
NCSC
neural crest stem cells
NS
neurospheres

Declarations

Ethics approval and consent to participate

This study has been performed with ethics approval by the Research Ethical Committee from the *Universitat Internacional de Catalunya*, under the study code BIO-ELB-2013-03 and all assays were adhered to the Declaration of Helsinki. Informed consent was obtained from donors after explanation of the use of the tissue.

Consent for publication

Not applicable

Availability of data and materials

The dataset supporting the conclusions of this article is included within the article

Competing interests

The authors declare not having competing interests.

Funding

This work was funded by the Government of Catalonia (2017 SGR 708), the Spanish Ministry (Ramón y Cajal fellowship (RYC2018-025977-I), predoctoral fellowship from Universitat Internacional de Catalunya (UIC) and Boehringer Ingelheim Fonds travelling grant.

Authors' contributions

BB and RN carried out the isolation and cell culture of stem cells. BB performed the cell reprogramming, cell differentiation and its analysis. ES and AS performed the corneal endothelial cell culture. FG and RA participated in the design of the study, participated in the manuscript writing and helped to draft the manuscript. All authors read and approved the final manuscript.

Acknowledgments

The authors thank the Center for Applied Medical Research (CIMA, University of Navarra) for the supply of fibroblasts and the Florida Lions Eye Bank (University of Miami Miller School of Medicine) for the supply of the corneoscleral rims.

References

1. Hatou S, Shimmura S. Review: corneal endothelial cell derivation methods from ES/iPS cells. *Inflamm Regen*. Springer Science and Business Media LLC; 2019;39.

2. Gain P, Jullienne R, He Z, Aldossary M, Acquart S, Cognasse F, et al. Global survey of corneal transplantation and eye banking. *JAMA Ophthalmol American Medical Association*. 2016;134:167–73.
3. Eye Bank Association of America [Internet]. 2018 [cited 2019 May 14]. Available from: <https://restoresight.org/eye-bank-association-america/>.
4. Joyce NC. Proliferative capacity of the corneal endothelium. *Prog. Retin. Eye Res*. 2003. p. 359–89.
5. Miyata K, Drake J, Osakabe Y, Hosokawa Y, Hwang D, Soya K, et al. Effect of donor age on morphologic variation of cultured human corneal endothelial cells. *Cornea*. 2001;20:59–63.
6. Senoo T, Joyce NC. Cell cycle kinetics in corneal endothelium from old and young donors. *Invest Ophthalmol Vis Sci*. 2000;41:660–7.
7. Joyce NC. Proliferative capacity of corneal endothelial cells. *Exp Eye Res*. 2012;95:16–23.
8. Katikireddy KR, Schmedt T, Price MO, Price FW, Jurkunas UV. Existence of Neural Crest-Derived Progenitor Cells in Normal and Fuchs Endothelial Dystrophy Corneal Endothelium. *Am J Pathol American Society for Investigative Pathology*. 2016;186:2736–50.
9. Okumura N, Okazaki Y, Inoue R, Kakutani K, Nakano S, Kinoshita S, et al. Effect of the rho-associated kinase inhibitor eye drop (Ripasudil) on corneal endothelial wound healing. *Investig Ophthalmol Vis Sci The Association for Research in Vision Ophthalmology*. 2016;57:1284–92.
10. Kinoshita S, Koizumi N, Ueno M, Okumura N, Imai K, Tanaka H, et al. Injection of cultured cells with a ROCK inhibitor for bullous keratopathy. *N Engl J Med*. 2018;378:995–1003.
11. Chakrabarty K, Shetty R, Ghosh A. Corneal cell therapy: With iPSCs, it is no more a far-sight. *Stem Cell Res. Ther. BioMed Central*; 2018. p. 287.
12. Wagoner MD, Bohrer LR, Aldrich BT, Greiner MA, Mullins RF, Worthington KS, et al. Feeder-free differentiation of cells exhibiting characteristics of corneal endothelium from human induced pluripotent stem cells. *Biol Open. Company of Biologists Ltd*; 2018;7.
13. Brejchova K, Dudakova L, Skalicka P, Dobrovolny R, Masek P, Putzova M, et al. iPSC-Derived corneal endothelial-like cells act as an appropriate model system to assess the impact of SLC4A11 variants on pre-mrna splicing. *Investig Ophthalmol Vis Sci. Association for Research in Vision and Ophthalmology Inc.*; 2019;60:3084–90.
14. Achilleos A, Trainor PA. Neural crest stem cells: discovery, properties and potential for therapy. *Cell Res Nature Publishing Group*. 2012;22:288–304.
15. Zhang W, Walboomers XF, Van Kuppevelt TH, Daamen WF, Van Damme PA, Bian Z, et al. In vivo evaluation of human dental pulp stem cells differentiated towards multiple lineages. *J Tissue Eng Regen Med. John Wiley & Sons, Ltd*; 2008;2:117–25.
16. Ferro F, Spelat R, Baheney CS. Dental pulp stem cell (DPSC) isolation, characterization, and differentiation. *Methods Mol Biol*. 2014. p. 91–115.
17. Lwigale PY. Corneal Development: Different Cells from a Common Progenitor. *Prog Mol Biol Transl Sci. Academic Press*; 2015. p. 43–59.

18. Syed-Picard FN, Du Y, Lathrop KL, Mann MM, Funderburgh ML, Funderburgh JL. Dental Pulp Stem Cells: A New Cellular Resource for Corneal Stromal Regeneration. *Stem Cells Transl Med.* Wiley-Blackwell; 2015;4:276–85.
19. Kushnerev E, Shawcross SG, Sothirachagan S, Carley F, Brahma A, Yates JM, et al. Regeneration of corneal epithelium with dental pulp stem cells using a contact lens delivery system. *Investig Ophthalmol Vis Sci The Association for Research in Vision Ophthalmology.* 2016;57:5192–9.
20. Liu Y, Jiang X, Zhang X, Chen R, Sun T, Fok KL, et al. Dedifferentiation-reprogrammed mesenchymal stem cells with improved therapeutic potential. *Stem Cells.* 2011;29:2077–89.
21. Núñez-Toldrà R, Montori S, Bosch B, Hupa L, Atari M, Miettinen S. S53P4 Bioactive Glass inorganic ions for Vascularized Bone Tissue Engineering by DPPSC Co-cultures. *Tissue Eng Part A.* 2019;ten.TEA.2018.0256.
22. Medvedev SP, Shevchenko AI, Zakian SM. Induced Pluripotent Stem Cells: Problems and Advantages when Applying them in Regenerative Medicine. *Acta Naturae.* 2010;2:18–28.
23. Llamas S, García-Pérez E, Meana Á, Larcher F, del Río M. Feeder Layer Cell Actions and Applications. *Tissue Eng Part B Rev Mary Ann Liebert Inc.* 2015;21:345–53.
24. Menendez L, Kulik MJ, Page AT, Park SS, Lauderdale JD, Cunningham ML, et al. Directed differentiation of human pluripotent cells to neural crest stem cells. *Nat Protoc.* 2013;8:203–12.
25. Kawano E, Toriumi T, Iguchi S, Suzuki D, Sato S, Honda M. Induction of neural crest cells from human dental pulp-derived induced pluripotent stem cells. *Biomed Res.* 2017;38:135–47.
26. Sabater AL, Andreu EJ, García-Guzmán M, López T, Abizanda G, Perez VL, et al. Combined PI3K/Akt and Smad2 activation promotes corneal endothelial cell proliferation. *Investig Ophthalmol Vis Sci The Association for Research in Vision Ophthalmology.* 2017;58:745–54.
27. Chen X, Wu L, Li Z, Dong Y, Pei X, Huang Y, et al. Directed differentiation of human corneal endothelial cells from human embryonic stem cells by using cell-conditioned culture media. *Investig Ophthalmol Vis Sci The Association for Research in Vision Ophthalmology.* 2018;59:3028–36.
28. Chen P, Chen J, Shao C, Li CY, Zhang YD, Lu WJ, et al. Treatment with retinoic acid and lens epithelial cell-conditioned medium in vitro directed the differentiation of pluripotent stem cells towards corneal endothelial cell-like cells. *Exp Ther Med.* 2015;9:351–60.
29. Gain P, Jullienne R, He Z, Aldossary M, Acquart S, Cognasse F, et al. Global survey of corneal transplantation and eye banking. *JAMA Ophthalmol American Medical Association.* 2016;134:167–73.
30. McCabe KL, Kunzevitzky NJ, Chiswell BP, Xia X, Goldberg JL, Lanza R. Efficient generation of human embryonic stem cell-derived corneal endothelial cells by directed differentiation. *PLoS One.* 2015;10:1–24.
31. Song Q, Yuan S, An Q, Chen Y, Mao FF, Liu Y, et al. Directed differentiation of human embryonic stem cells to corneal endothelial cell-like cells: A transcriptomic analysis. *Exp Eye Res Elsevier Ltd.* 2016;151:107–14.

32. Janebodin K, Horst OV, Ieronimakis N, Balasundaram G, Reesukumal K, Pratumvinit B, et al. Isolation and characterization of neural crest-derived stem cells from dental pulp of neonatal mice. *PLoS One Public Library of Science*. 2011;6:e27526.
33. Kim JB, Zaehres H, Araúzo-Bravo MJ, Schöler HR. Generation of induced pluripotent stem cells from neural stem cells. *Nat Protoc Nature Publishing Group*. 2009;4:1464–70.
34. Chen M-J, Lu Y, Hamazaki T, Tsai H-Y, Erger K, Conlon T, et al. Reprogramming adipose tissue-derived mesenchymal stem cells into pluripotent stem cells by a mutant adeno-associated viral vector. *Hum Gene Ther Methods Mary Ann Liebert Inc*. 2014;25:72–82.
35. Sun N, Panetta NJ, Gupta DM, Wilson KD, Lee A, Jia F, et al. Feeder-free derivation of induced pluripotent stem cells from adult human adipose stem cells. *Proc Natl Acad Sci U S A National Academy of Sciences*. 2009;106:15720–5.
36. Zhang S, Lv Z, Zhang S, Liu L, Li Q, Gong W, et al. Characterization of human induced pluripotent stem cell (iPSC) line from a 72 year old male patient with later onset Alzheimer's disease. *Stem Cell Res Elsevier BV*. 2017;19:34–6.
37. Zapata-Linares N, Rodriguez S, Mazo M, Abizanda G, Andreu EJ, Barajas M, et al. Generation and characterization of human iPSC line generated from mesenchymal stem cells derived from adipose tissue. *Stem Cell Res Elsevier BV*. 2016;16:20–3.
38. Bajpai R, Chen DA, Rada-Iglesias A, Zhang J, Xiong Y, Helms J, et al. CHD7 cooperates with PBAF to control multipotent neural crest formation. *Nature NIH Public Access*. 2010;463:958–62.
39. Baker M. Embryoid bodies get organized. *Nat Reports Stem Cells*. 2008.
40. Xiong F, Gao H, Zhen Y, Chen X, Lin W, Shen J, et al. Optimal time for passaging neurospheres based on primary neural stem cell cultures. *Cytotechnology Springer*. 2011;63:621–31.
41. Green SA, Simoes-Costa M, Bronner ME. Evolution of vertebrates as viewed from the crest. *Nature*. Nature Publishing Group; 2015. p. 474–82.
42. Elkabetz Y, Panagiotakos G, Al Shamy G, Socci ND, Tabar V, Studer L. Human ES cell-derived neural rosettes reveal a functionally distinct early neural stem cell stage. *Genes Dev*. Cold Spring Harbor Laboratory Press; 2008;22:152–65.
43. Shen L, Sun P, Zhang C, Yang L, Du L, Wu X. Therapy of corneal endothelial dysfunction with corneal endothelial cell-like cells derived from skin-derived precursors. *Sci Rep Nature Publishing Group*. 2017;7:13400.
44. Lachaud CC, Soria F, Escacena N, Quesada-Hernández E, Hmadcha A, Alió J, et al. Mesothelial cells: A cellular surrogate for tissue engineering of corneal endothelium. *Investig Ophthalmol Vis Sci The Association for Research in Vision Ophthalmology*. 2014;55:5967–78.
45. Yamashita K, Inagaki E, Hatou S, Higa K, Ogawa A, Miyashita H, et al. Corneal endothelial regeneration using mesenchymal stem cell derived from human umbilical cord. *Stem Cells Dev*. 2018;27.

Figures

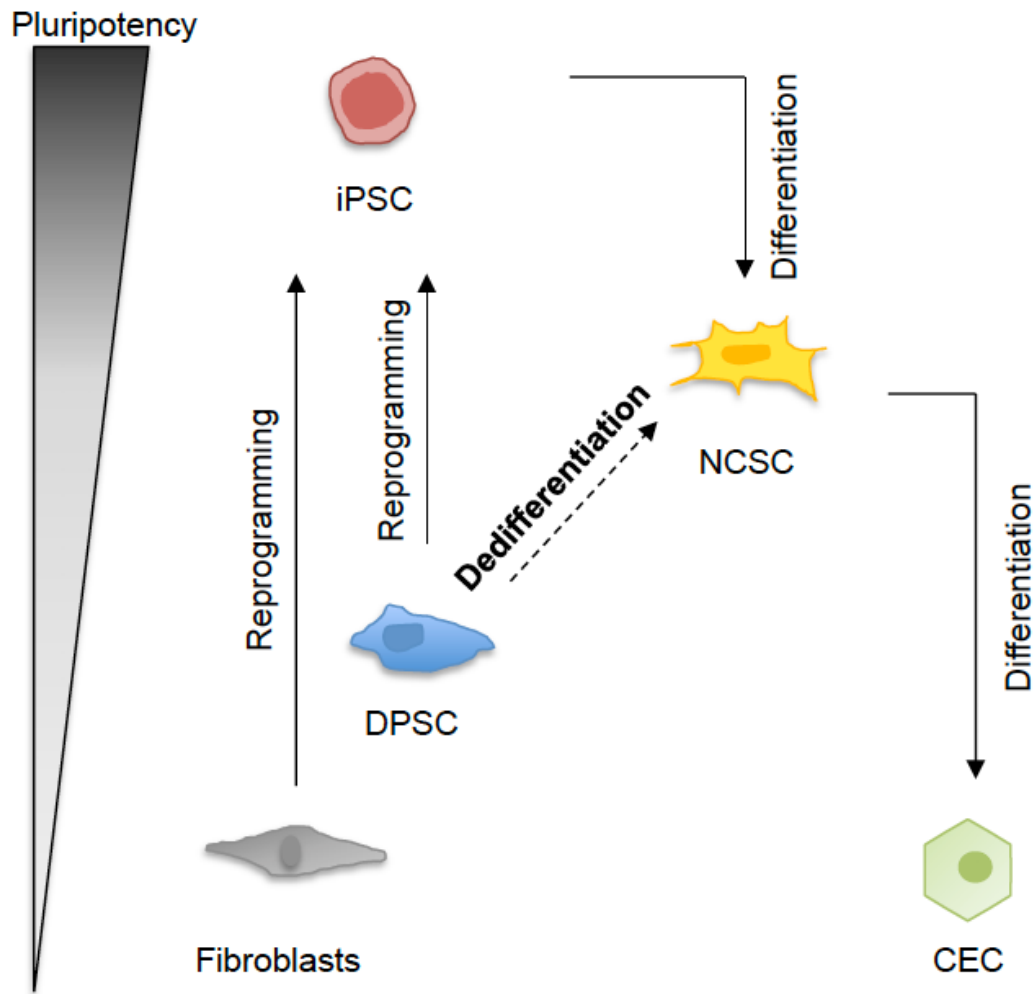


Figure 1

Schematic representation of corneal endothelial differentiation based on the pluripotency levels. On the one hand, somatic cells as fibroblasts and DPSC can be reprogrammed into iPSC, which can be differentiated into NCSC and then into CEC. On the other hand, DPSC could be dedifferentiated into NCSC, and then differentiated into CEC.

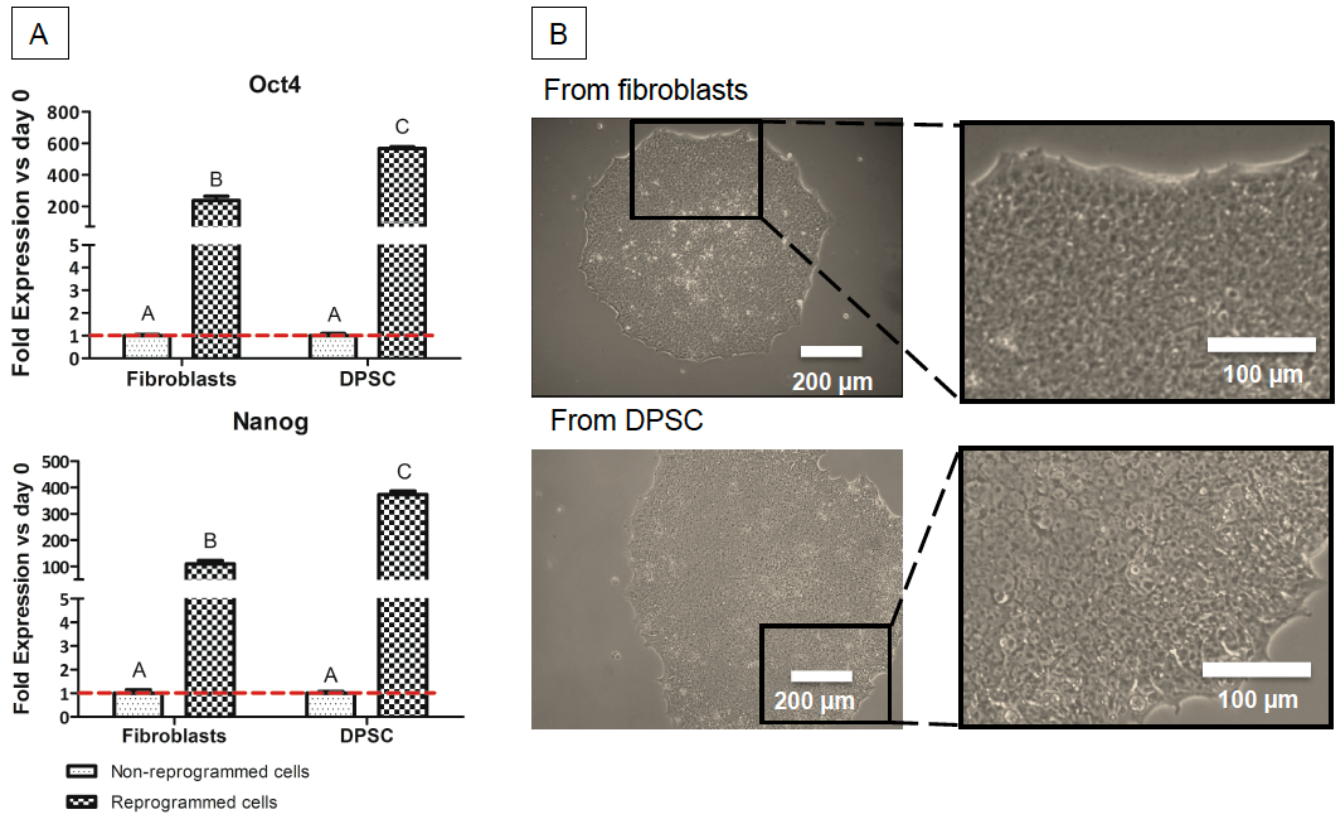


Figure 2

Cell reprogramming from DPSC and fibroblasts. Relative mRNA expression in DPSC and fibroblasts (positive control), before and after cell reprogramming (A). Pluripotent expression of Oct 4 and Nanog by quantitative RT-PCR. Optical microscope images of iPSC colonies cultured in VTN-coated dishes from fibroblasts (positive control) and from DPSC (B). *Scale bars: 200 μ m (lower magnification) and 100 μ m (higher magnification). **Different letter denotes significant differences. Same letter denotes non-significant differences.

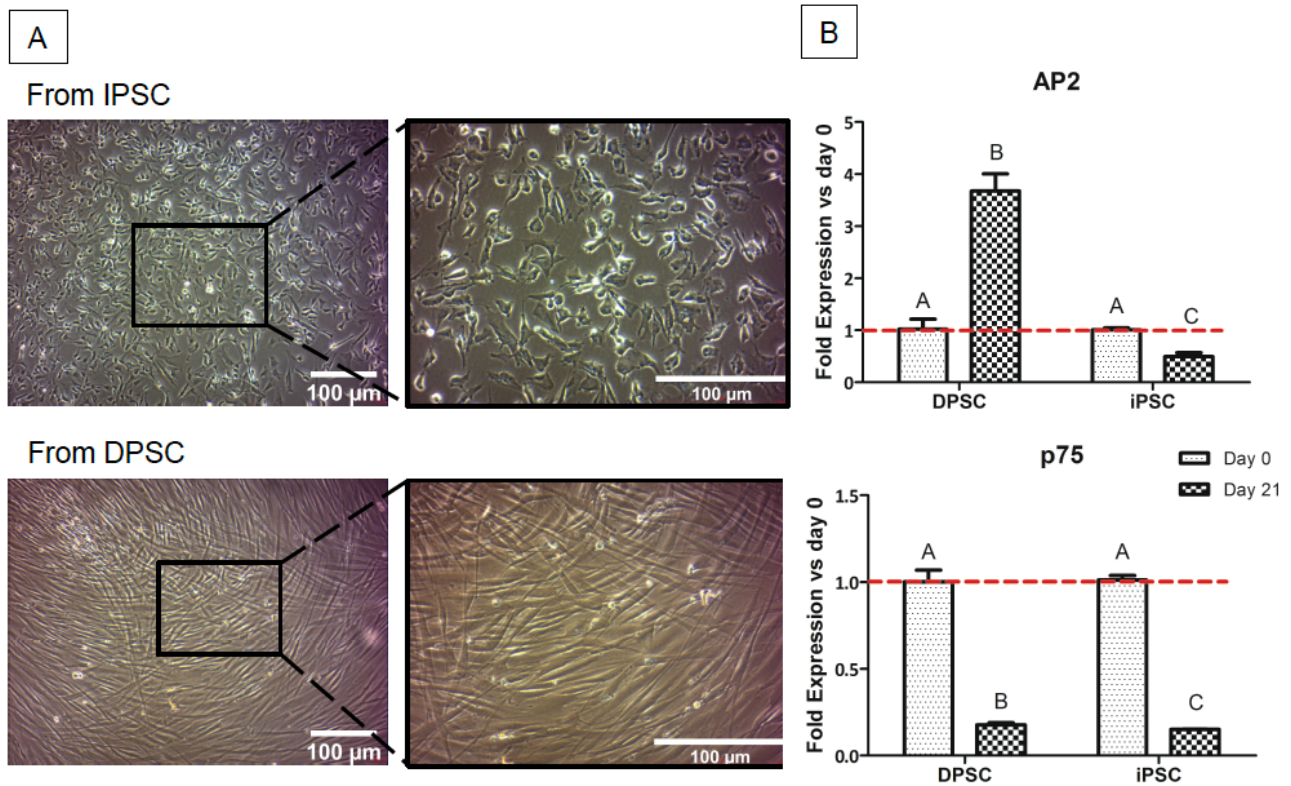


Figure 3

Formation of NCSC using an adherent method. Microscope images of NCSC-derived from iPSC and from DPSC at day 21 of differentiation (A). Relative mRNA expression in NCSC-derived from DPSC and iPSC, at days 0 and 21 (B). NCSC expression of AP2 and p75 by quantitative RT-PCR. *Scale bar: 100 μ m.

**Different letter denotes significant differences. Same letter denotes non-significant differences.

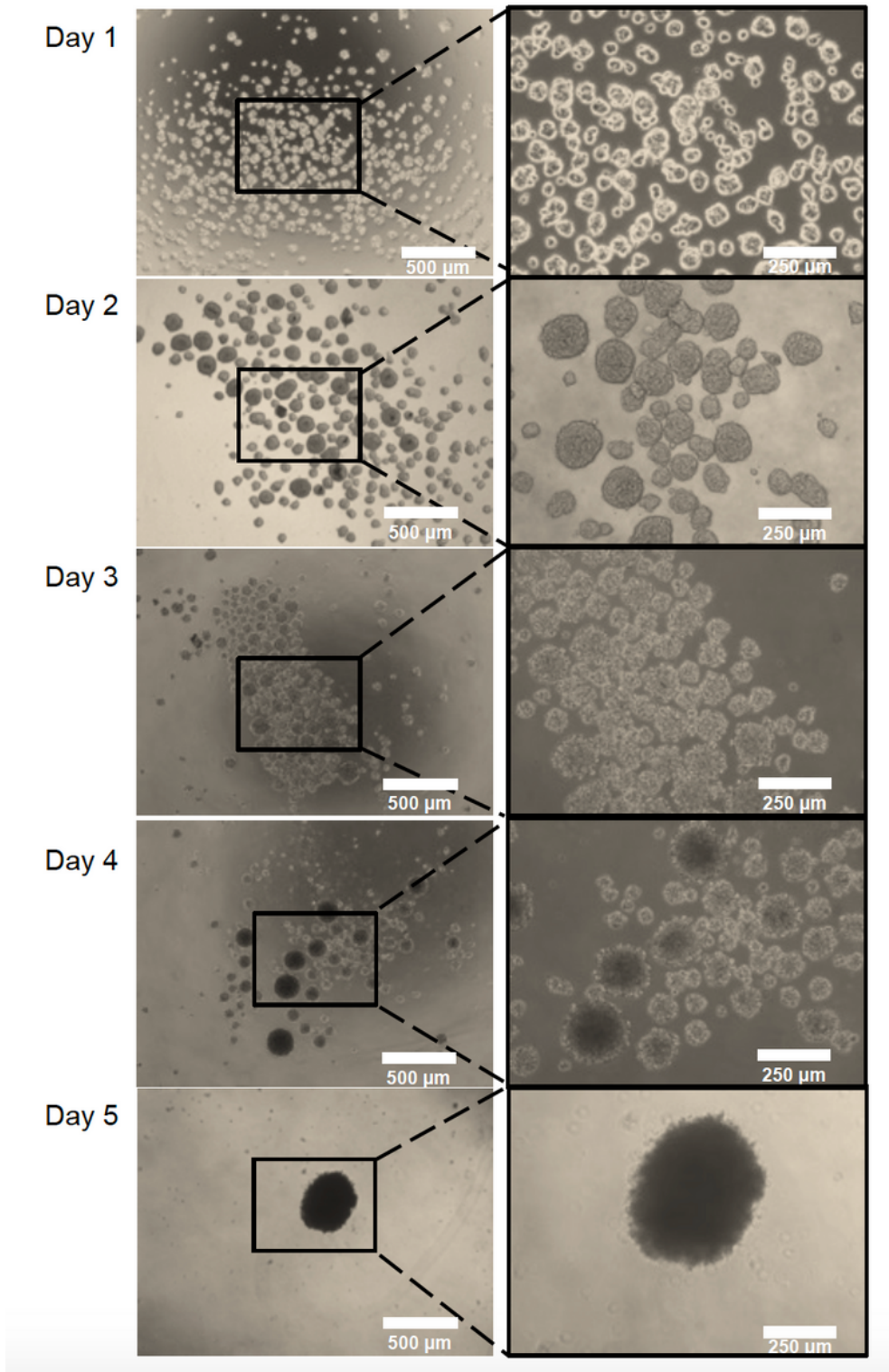


Figure 4

Formation of NCSC from DPSC using a suspension method. Microscope images of cell morphology at days 1, 2, 3, 4 and 5 of NCSC formation in suspension culture. Scale bars: 500 μm (lower magnification) and 250 μm (higher magnification).

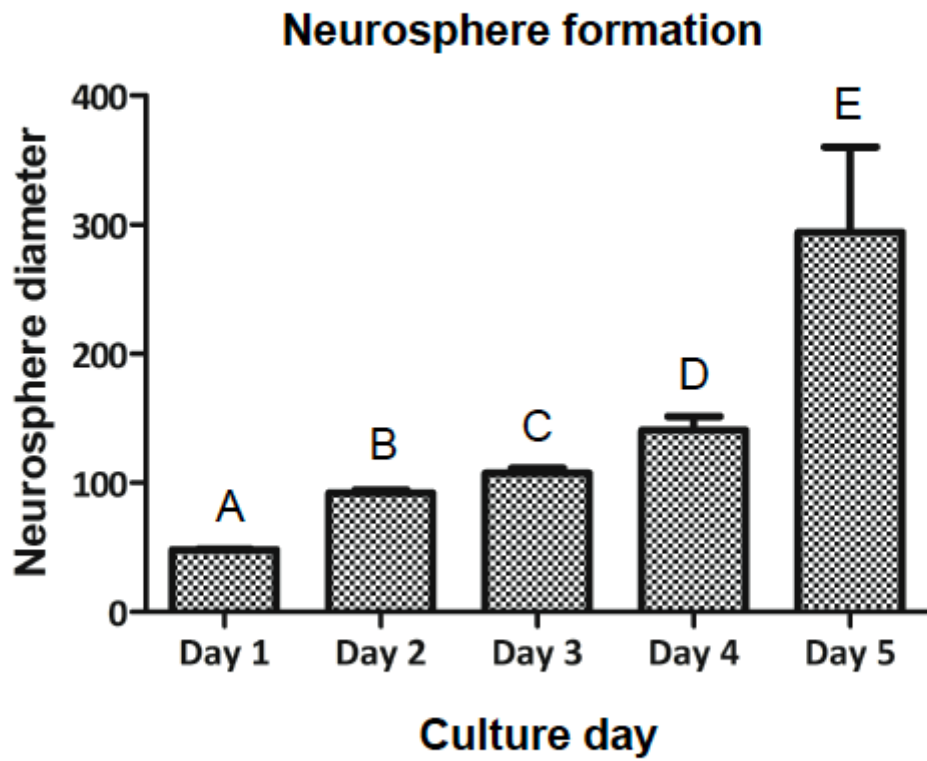


Figure 5

Neurosphere diameter at days 1-5 of suspension culture.

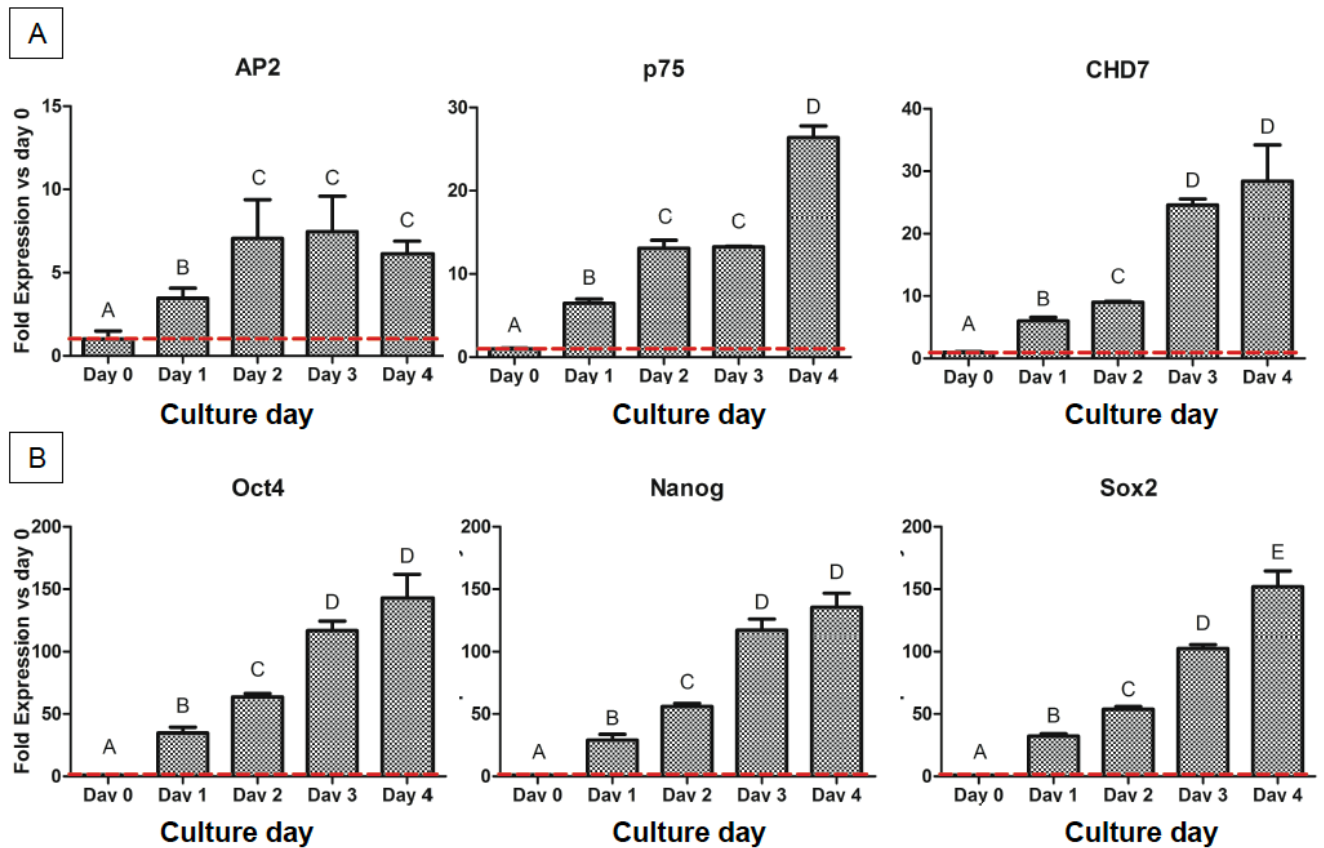


Figure 6

Gene expression of NCSC formation from DPSC in suspension culture. Relative mRNA expression of NCSC markers AP2, p75 and CHD7 (A) and pluripotent markers Oct4, Nanog and Sox2 (B) analyzed by quantitative RT-PCR. * Different letter denotes significant differences. Same letter denotes non-significant differences.

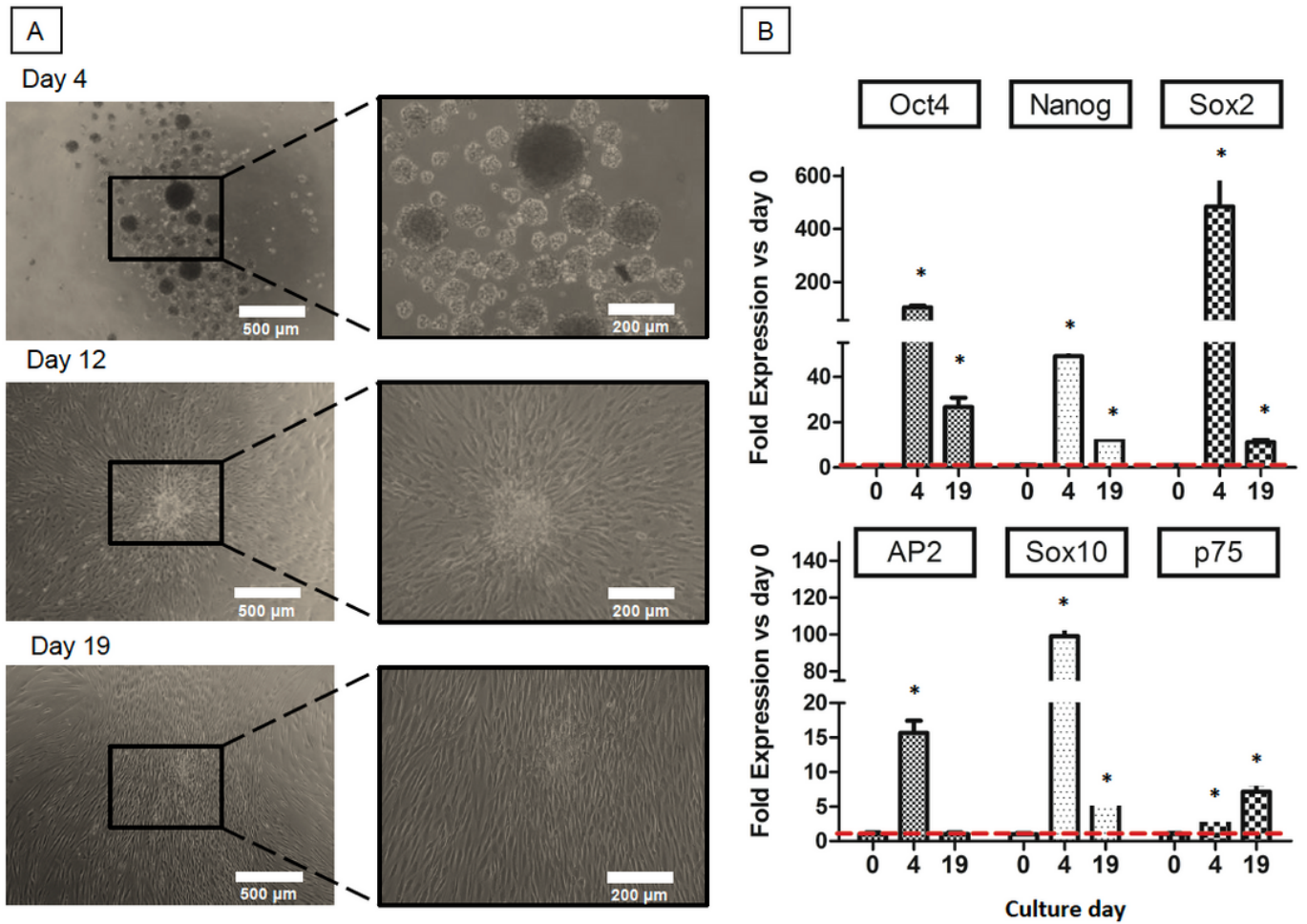


Figure 7

Expansion of NCSC from DPSC. Microscope images of NCSC-derived from DPSC at days 4, 12 and 19 (A). Relative mRNA expression in NCSC-derived from DPSC, at days 0, 4 and 19 of NCSC markers AP2, Sox10 and p75, and of pluripotent markers Oct4, Nanog and Sox2, by quantitative RT-PCR (B). *Scale bars: 500 μm (lower magnification) and 200 μm (higher magnification). * Significant differences compared to day 0.

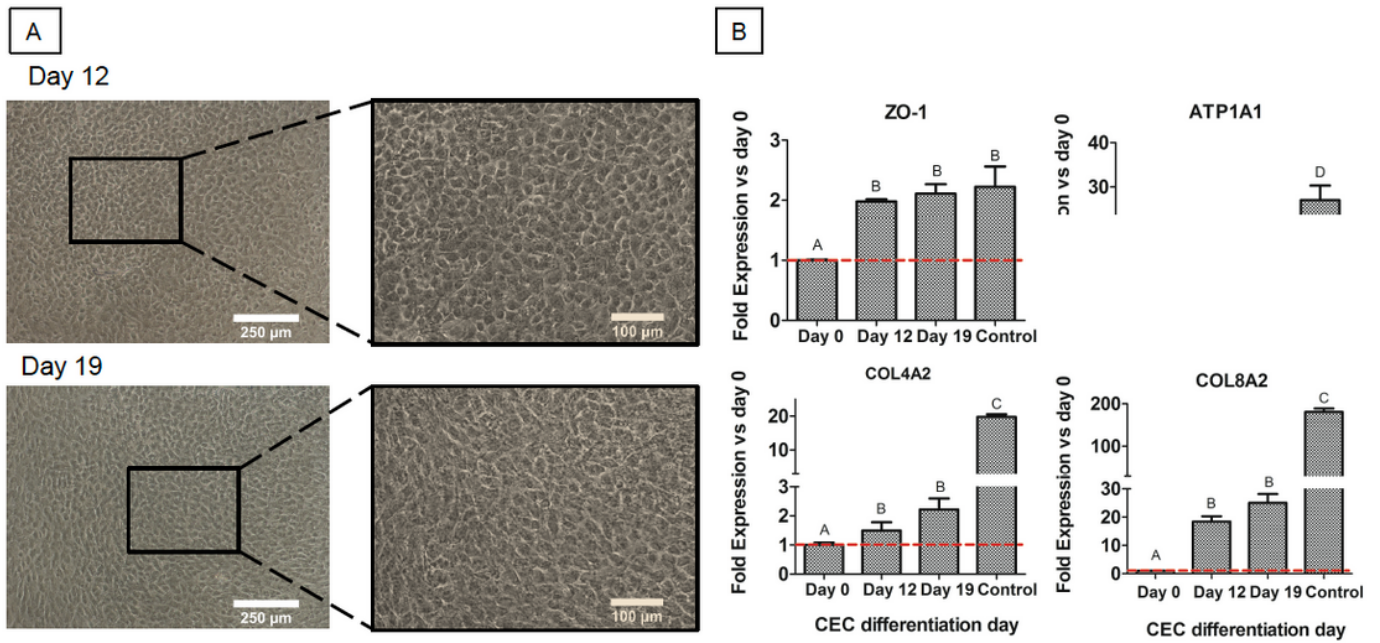


Figure 8

CEC differentiation from DPSC. Microscope images of CEC-derived from DPSC at days 12 and 19 (A). Relative mRNA expression in CEC-derived from DPSC, at days 0, 4 and 19 of CEC markers ZO-1, ATP1A1, COL4A2 and COL8A2, by quantitative RT-PCR (B). *Scale bars: 250 μm (lower magnification) and 100 μm (higher magnification). **Different letter denotes significant differences. Same letter denotes non-significant differences